

Ocean temperature controls help decomposition and carbon sink potential

Karen Filbee-Dexter (✉ kfilbeedexter@gmail.com)

Institute for Marine Research <https://orcid.org/0000-0001-8413-6797>

Colette Feehan

Dalhousie University

Dan Smale

Marine Biological Association of the United Kingdom <https://orcid.org/0000-0003-4157-541X>

Kira Krumhansl

Bedford Institute of Oceanography, Fisheries and Oceans Canada

Skye Augustine

Simon Fraser University

Florian de Bettignies

Station Biologique de Roscoff, Sorbonne University

Michael T. Burrows

Scottish Association For Marine Science

Jarrett Byrnes

University of Massachusetts Boston

Jillian Campbell

Simon Fraser University

Dominique Davoult

Sorbonne Université, CNRS, UMR 7144, Station Biologique

Kenneth Dunton

The University of Texas at Austin

Joao Franco

Marine and Environmental Sciences Centre

Ignacio Garrido

Laval University

Sean Grace

Southern Connecticut State University <https://orcid.org/0000-0002-5437-0782>

Kasper Hancke

Norwegian Institute for Water Research

Ladd Johnson

Laval University

Brenda Konar

University of Alaska Fairbanks

Morten Pedersen

Roskilde University

Pippa Moore

IBERS <https://orcid.org/0000-0002-9889-2216>

Kjell Magnus Norderhaug

Institute of Marine Research

Alasdair O'Dell

Scottish Association for Marine Science

Anne Salomon

Simon Fraser University

Isabel Sousa-Pinto

University of Porto

Dara Yiu

Montclair State University

Thomas Wernberg

University of Western Australia <https://orcid.org/0000-0003-1185-9745>

Article

Keywords:

Posted Date: July 15th, 2020

DOI: <https://doi.org/10.21203/rs.3.rs-38503/v1>

License:   This work is licensed under a Creative Commons Attribution 4.0 International License.

[Read Full License](#)

Abstract

Compelling new evidence shows that kelp production contributes an important and underappreciated flux of carbon in the ocean. Major questions remain, however, about the controls on the cycling of this organic carbon in the coastal zone, and their implications for future carbon sequestration. Here we used field experiments distributed across 28° latitude, and the entire range of two dominant kelps in the northern hemisphere, to measure decomposition rates of kelp detritus on the seafloor in relation to environmental factors. Ocean temperature was the strongest control on detritus decomposition in both species, and it was positively related to decomposition. This suggests that decomposition could accelerate with ocean warming under climate change, increasing remineralization and reducing overall kelp carbon sequestration. However, we also demonstrate the potential for high kelp-carbon storage in cooler (northern) regions, which could be targeted by climate mitigation strategies to expand blue carbon sinks.

Introduction

The cycling of organic carbon in the ocean is a critical yet unresolved component of the global carbon cycle^{1,2}. Consequently, there has been a strong focus on resolving inorganic carbon (CO₂) uptake and primary productivity on global scales³. Yet, decomposition rates of organic carbon at the ecosystem scale, which are known to vary with environmental conditions such as temperature^{e.g., 4,5}, could be equally important in determining the balance between pools of organic and inorganic carbon^{6–8}. At the land-sea interface, carbon cycling by macroalgae and other macrophytes has recently emerged as an important process by which CO₂ is captured, stored, and potentially sequestered in the ocean^{9,10}. As such, quantifying rates of decomposition of macroalgal detritus in the marine environment is essential to estimate its potential contribution to blue carbon¹¹ and its fate in the global carbon cycle more generally.

Decomposition rates of organic carbon vary geographically, and this is a challenge for current climate models, which usually use spatially uniform relationships to represent major processes or pathways^{1,12–14}. On land, models that consider spatiotemporal dependencies in temperature, microbial, and mineral surface interactions predict weaker and more variable soil-carbon–climate feedbacks than models using average rates¹⁵. In the open ocean, the global biological pump has large regional variability, with particulate organic carbon (POC) decomposition rates ranging over two orders of magnitude. As a result of these spatial differences, commonly applied rates of POC decomposition based on measures from a few areas have overestimated the global flux of POC to the seafloor¹⁶. Similarly, variation in deep sea benthic communities appears to drive strong heterogeneity in carbon turnover rates following deposition¹ and latitudinal differences in microbial activity are expected to drive slower degradation rates of dissolved organic carbon at higher latitudes⁴.

The dynamics of temperature-decomposition relationships are also complex¹⁷. Organic matter tends to be remineralized faster in warmer compared to cooler environments, and the temperature-dependent decomposition of carbon has been highlighted as a key source of uncertainty in future global carbon

models^{5,18,19}. Understanding the environmental drivers underlying spatial variation in carbon turnover is critical because it effectively controls how current rates of carbon cycling could be changed with global warming. In particular, it informs whether environmental and biological changes will create positive feedbacks on the entire carbon cycle that lead to further warming, as opposed to negative feedbacks that buffer impacts and buy time to reduce emissions.

Large brown macroalgae at high latitudes form kelp forests, which assimilate substantial quantities of CO₂ by virtue of their exceptional productivity and large spatial extent^{20,21}. Many kelp forests are declining globally, particularly in regions with high seawater temperatures and rapid warming^{22–25}. In contrast, kelp forests in cooler regions are relatively stable, and in some cases kelp is even increasing in abundance^{24,26–29}. Changes in the abundance of kelp, and the environmental conditions they experience, may have consequences for the global carbon cycle. More than 80% of kelp production enters the coastal ecosystem as detritus, where it eventually strands on beaches, sinks to the seafloor, or is decomposed^{20,30}. In general, the slower the decomposition of kelp detritus in the ocean, the greater chance it has for sequestration in the deep ocean and the longer it takes to re-enter the atmosphere as CO₂^{16,31}. For example, macroalgal detritus that reaches open ocean depths >1000 m is considered trapped in water masses where the CO₂ is retained for significant time periods (i.e., >1000 years) before returning to the ocean surface and eventually the atmosphere^{9,32}. Detritus that is retained in some nearshore areas, such as deep fjords or basins with high rates of sedimentation may also be buried for 100s to 1000s of years, effectively removing it from the short-term carbon cycle^{33–36}.

Here we conducted a broadly distributed field experiment at 35 sites spanning 12 geographic regions across the northern hemisphere (Fig. 1) to measure decomposition rates of kelp detritus in coastal habitats and to assess the influence of an ocean climate gradient on decomposition. Experiments on two dominant species of kelp (*Laminaria hyperborea* and *Saccharina latissima*) were deployed through a collaborative network of researchers in the northeast Pacific Ocean (n = 1), the subarctic Norwegian Sea (n = 1), the Gulf of Alaska (n = 1), the northeast Atlantic Ocean (n = 4), and the northwest Atlantic Ocean (n = 5). Our study sites spanned 28° in latitude, 169° in longitude, and encompassed the entire distribution of the two kelp species and a gradient in mean sea temperature of ~14°C. We hypothesized that the large spatial range in environmental conditions would drive significant differences in kelp-carbon decomposition rates, and that turnover would be faster in areas with warmer temperature, lower light, and higher water movement.

Results

Our study regions experienced markedly different temperature conditions, with average temperatures ranging from 6 to 21 °C and regional minimum and maximum temperatures spanning from 2 to 24 °C, over the 4 to 18-week study (Fig. 1).

Across all our study regions, kelp biomass decomposed at an average rate of $0.74 \pm 0.87 \% d^{-1}$ (\pm SD) reaching 50 % loss after 67 days, on average. Decomposition rates for both species were inversely related to latitude along the 28° gradient (Fig. 2). The most rapid biomass loss occurred at the southernmost sites in Rhode Island Sound, USA ($1.76 \pm 0.39 \% d^{-1}$) and Portugal ($2.63 \pm 0.66 \% d^{-1}$). Biomass loss was similar among the Norwegian Sea, the Gulf of Alaska, and other regions in cooler parts of the northeast Atlantic Ocean, with extremely slow decomposition rates ($0 - 0.28 \% d^{-1}$) over the 72 - 121 d duration of the experiment, and evidence that kelp detritus continued to grow after deployment, especially in the Norwegian Sea and Gulf of Alaska (Fig. 2).

We used generalized linear mixed models to describe relationships between decomposition rates and environmental conditions on the seafloor (water temperature [average and range], light, water movement), as well as algal material traits (species, % carbon), while accounting for study region and site (Table 1, Supplementary Table 2). These models showed a significant positive relationship between kelp decomposition rate and average water temperature (Fig. 3a), which explained 72% of the variation of all fixed and random effects, suggesting that the observed patterns were largely driven by sea temperature. There was a negative correlation between average temperature and latitude across our study sites (Pearson's $R = -0.59$, $p < 0.001$, $n = 35$), but there was variation around this trend due to the influence of factors independent of latitude on temperature, such as ocean currents (e.g., Gulf Stream and Labrador Currents). We found no evidence that differences in water movement or light intensity influenced kelp decomposition, which we expected would either increase mechanical breakdown or delay tissue death by maintaining low levels of photosynthesis. Average light intensity was highly variable across the study regions (range 10 – 100 Lux), but average water movement was similar (range $0.98 - 1.15 g^3$), likely due to consistent wave dampening by the cages which could explain its low importance in the model.

The two kelp species had different decomposition rates, with *S. latissima* losing biomass significantly faster than *L. hyperborea* (Fig. 3b, Table 1). Decomposition rates were more variable among regions than among sites within regions suggesting that heterogeneity in local conditions did not influence the larger spatial patterns in decomposition (Table 1). Initial % carbon content also had a significant effect on the decomposition rates during the experiment, with slower decomposition rates for detritus with higher carbon content (Table 1, Fig. 3c).

Over the experiment, the average nitrogen content increased significantly in both *S. latissima* and *L. hyperborea* detritus in some regions (*S. latissima*: France and Rhode I Sound; *L. hyperborea*: France and Scotland), suggesting that the kelp tissue became nitrogen enriched as it underwent degradation in these regions (Fig. 4), possibly via increased microbial abundance or activity. We did not detect a relationship between changes in kelp tissue composition (C:N or % nitrogen) and temperature, light, or water movement over the course of the experiment (Supplementary Table 3). The nitrogen content in kelp tissue at the onset of the study was highly variable among regions (Fig. 4), which likely reflects different background nutrient levels or initial kelp condition.

Discussion

Our experiments revealed a significant relationship between temperature and kelp detritus decomposition rates across the northern hemisphere, with markedly slower decomposition in cooler northern regions relative to warmer southern regions. Temperature dependence of organic-matter decomposition constitutes an important link between climate change and the global carbon cycle⁵, including in the ocean where there are large actively cycling pools of organic matter^{38,39}. There is a widely held view that decomposition rates and carbon turnover are faster at lower latitudes, due to increased microbial activity and metabolic rates of detritivores in warmer climates^{8,17,40}. However, empirical evidence shows that these patterns do not hold in many systems, and such temperature relationships may not be universal^{41–45}. Nevertheless, these relationships have important implications for potential positive feedbacks of climate change, and they underpin predictions of increased permafrost decomposition from microbial activity⁷ and faster soil degradation from increased decomposer activity^{6,46} with global warming. The present study shows that such a relationship exists for kelp detritus on a large spatial scale. Our study also identifies cool regions as possible hotspots for kelp carbon storage and sequestration by providing evidence that kelp detritus in these regions remains intact for longer, increasing its dispersal potential to carbon sinks⁴⁷. This potentially has important consequences for global patterns of carbon cycling in the coastal zone.

The temperature-dependent rates of kelp decomposition uncovered here suggest that future kelp detritus turnover will become more rapid as coastal zones warm. Faster turnover means that detritus will have shorter residence time and lower potential to be exported and transported to deep marine sediments or water bodies or sequestered by burial in shallow soft sediments^{9,47}. This would imply a loss of potential carbon sequestration within the current distribution of kelp forests *e.g.*,⁴⁸ under future warming. This change would also alter the nature of kelp as a resource subsidy, which will have ramifications for detrital food webs within the kelp forests and in adjacent habitats that rely on this source of production²⁰.

Importantly, although decomposition varied across regions, kelp detritus decomposed slower than many other dominant sources of organic carbon in the ocean (*e.g.*, zooplankton casings, feces and debris, phytodetritus, bacteria), and at rates similar to other forms of benthic vegetation (*e.g.*, seagrass and other seaweeds) (Table 2). This could be related to the physicochemical properties of kelp material, such as the presence of structural compounds and phenols⁴⁹. Also, it could be because the material, even as detritus, can remain viable and photosynthetically active for extended periods in shallow subtidal areas with sufficient light to maintain net photosynthesis⁵⁰. Although critical information about export of this detrital material is still lacking in many regions¹¹, our findings show that kelp detritus has long residence times in the coastal zone, and therefore high potential to be transported to deeper regions^{36,47}. This is consistent with evidence that a substantial amount of kelp reaches deep marine sinks where it can be sequestered in the long-term^{11,32,51}.

We found a significant negative relationship between initial carbon content in detritus and decomposition rate, which could indicate that more carbon-rich tissue was less palatable to microorganisms or detritivores. This is supported by other studies showing detritus quality is a key predictor of decomposition^{52,53}. The nitrogen enrichment of detritus that occurred in some regions may be explained by increased microbial colonization^{54,55}. However, we detected no relationship between nitrogen enrichment and temperature over the course of the experiment. This finding differs from those of distributed decomposition experiments in freshwater systems that suggest warmer temperature shifts decomposition from detritivore to microbial pathways⁵³.

Kelp forests are currently changing in distribution and abundance due to climate change^{21,24}, with implications for the storage and cycling of kelp carbon. *S. latissima* and *L. hyperborea* are disappearing at their warmer southern range edges^{56–58}. Kelp forests in other north Atlantic regions, such as around the British Isles, have undergone structural changes following climate-driven shifts in kelp species distributions⁵⁹, also leading to concomitant shifts in rates and timings of carbon fixation and release⁶⁰. Along the west coast of North America, loss of predators and marine heatwaves are driving shifts from kelp forests to sea urchins barrens in some areas^{61–63}. Our findings imply an overall reduction in rates of kelp carbon decomposition as oceans warm, which represents faster carbon cycling and lost storage potential. However, the predicted expansion of kelp forests along Arctic coasts due to reduced sea ice⁶⁴ could lead to extensive and more productive kelp forests in cooler regions, where decomposition rates are slower and long term carbon sequestration more likely^{27,64, but see 65}. The consistent changes in decomposition across latitudes highlights the issues with representing major processes underpinning carbon cycling in the ocean in a uniform manner across space. While these patterns should be better understood, incorporating them into estimates of carbon cycling in a future ocean will improve current predictions and better resolve the climate mitigation potential of kelp forests. Indeed, understanding key processes such as decomposition at the ecosystem level should lead to a fuller understanding of carbon cycling on a global scale.

Methods

Fieldwork and laboratory analyses were conducted by a collaborative network covering the global range of two dominant and broadly distributed kelp species (*S. latissima* and *L. hyperborea*) (Fig. 1). Field decomposition rates of kelp detritus were quantified in concurrent, standardized litterbag experiments deployed in 12 regions throughout the northern hemisphere. Litterbag experiments are widely used to quantify decomposition rates in the field⁶⁶ by measuring the mass loss of plant material enclosed in mesh bags that allow water flow and microbial colonization while excluding large grazers and preventing biomass advection. In each region, three sites, approximately 0.5 to 10 km apart, were selected on sand or coarse sediment adjacent to rocky reefs in areas with low to moderate wave and current exposure (Supplementary Table 1). Litterbags were pre-assembled and shipped to all partners, ensuring identical treatments were deployed in all regions. We targeted overall patterns of kelp loss rather than attempting to distinguish between mesograzers (or detritivores) and microbial activity. Consequently, we did not vary

mesh size of the litterbags as this can substantially alter light and water flow, which may affect kelp decomposition.

In each of the 12 regions divers haphazardly collected 24 adult blades with minimal to no epibionts of each targeted species. Six regions collected and deployed two species (*S. latissima* and *L. hyperborea*), and six regions deployed one species (*S. latissima*) (Supplementary Table 1). From each blade a 20-g piece of kelp tissue was sectioned ~15 cm from the base and at least 15 cm from the distal end and weighed to the nearest 0.01 g. This approach was chosen to maximize blade uniformity across regions as older distal tissue would be less uniform depending on age and fouling. Using newly formed basal tissue also minimized phenological or seasonal differences in detrital material from slight variation in timing of the trials across regions, which may influence the decomposition rates. Additional kelp samples (n = 8-10) were collected for each species for baseline C:N analyses.

A single kelp piece was loosely packed into each litterbag (plastic ~1 x 1-cm mesh bags) and placed into cages (four litterbags in each of the two cages for each species at each site), to allow access of smaller mesograzers. Cages were 20 cm by 20 cm by 40 cm and made of plastic 1 x 1 cm mesh ('gutter guard'). Each cage was tethered with cable ties to a weight on the seafloor at ~8-m depth. In order to accurately quantify the impact of ocean climate on decomposition, we selected this cage size to exclude grazing by large herbivores in our experiments, which can drive localized increases in the turnover, size, and availability of kelp detritus in some areas³⁶ and could overwhelm measures of turnover in areas where they were locally abundant. All kelp pieces were kept damp after collection, stored in a dark cooler and deployed within 24 hours of collection.

Environmental variables known to influence decomposition were measured concurrently throughout the experiment at each site. Hourly light and temperature were measured by an Onset HOB0 pendant temperature and light logger fixed to the top of a cage at each site. Only light records for the first two weeks of deployment were used to account for fouling of the sensor, which could shade and confound measurements over time. To estimate wave action, an Onset HOB0 G logger was placed inside a mesh bag and added to a cage at each site to log hourly movement of the litterbags. We used the average product of logged acceleration along 3 axes (x, y and z, units of g³) of the period as a relative measure of movement of the litterbags.

Approximately 4-6 weeks into the experiment half the litterbags were collected (two from each cage). The remaining litterbags were collected after 12-18 weeks. Litterbags were lost at some sites (Supplementary Table 1). Samples were processed within 10 h of collection. All kelp fragments were removed from bags, patted dry, and weighed to the nearest 0.01 g. Weighed samples were rinsed in distilled water, oven dried at 60 °C for 48 h, and then shipped to the University of California (Davis, CA, USA) where they were analyzed for nitrogen and carbon tissue content.

We compared the obtained values of kelp decomposition to that of other marine detritus using data from litterbags or incubations obtained from the literature (Supplementary Table 4). For each type of organic

material (seaweed, seagrass, mangrove, other particulate detritus (e.g., marine snow, zooplankton feces or debris), and dissolved organic material (DOM)) we calculated residence times (days to 50% loss). This metric enabled comparison between materials with different decay functions. We did not include refractory pools of DOM or below-ground decomposition.

Analysis

Rates of kelp loss (average rate of biomass loss for each retrieval time at each site) as a function of environmental conditions and kelp tissue properties were analyzed by generalized linear mixed effects models. Sites were averaged because litterbags in the same cage were not independent replicates. We also calculated k values, using the equation $y = e^{-kt}$, where y is the proportion of biomass remaining at a time point and t is the time elapsed since the beginning of the experiment (days), but linear rates of loss fit our dataset better. The lagged onset of decomposition in some of our study regions may explain why our linear decomposition rates, although similar to other regional decomposition experiments on kelp detritus^{50,55}, deviated from patterns of exponential decay shown for other types of organic material⁶⁷. Because we were examining kelp decomposition, any negative rates of loss (biomass increase or growth) were assigned a value of 0 in our model, as a growing kelp is undergoing little to no decomposition. This was important for sites in the subarctic, where kelp detritus continued to grow after deployment. Our predictor variables were obtained from logger data and stable isotope measures. The fixed effects were kelp species, average water temperature, range in water temperature, average light conditions, and relative water movement during the experimental period, as well as site nested within region as the random effects. We used two variables to capture temperature conditions, the average temperature over the deployment and the temperature range (the difference between the 10th and 90th percentiles) as temperature ranges varied markedly, from 0.6 to 18.6 °C. Average temperatures and peak temperatures (90th percentile) were highly correlated among sites (Pearson's $R = 0.96$, $p < 0.001$), so peak temperatures were not included in our model. Temperature loggers were lost in the Gulf of Maine region, so temperatures were obtained from the closest meteorological weather buoy (19 km away).

We accounted for differences in starting kelp conditions using initial % carbon content in kelp tissue as fixed effects in the model. This variable was correlated with initial % nitrogen and C:N ratio (Pearson's correlation tests, $R > 0.7$), so only initial % carbon was included in the model. Carbon content was modelled separately using a subset of the data, because these measures were not available for Gulf of Maine, Rhode I Sound, and the Gulf of St Lawrence. The main relationships between the other key variables (light, temperature, species) were similar in both models. To confirm the latitudinal gradient was statistically significant, we ran another model using the continuous variable of 'latitude' as a predictor of biomass loss instead of a categorical variable (region name) (Supplementary Information 1). We did not use 'latitude' in our final model because it was correlated with temperature and the environmental gradients underlying these latitudinal differences provided more interesting and operational information on spatial patterns of carbon turnover.

We tested for significant nitrogen enrichment of *S. latissima* and *L. hyperborea* using a 2-way ANOVA comparing %N at the start and end of the experiment among regions. Post-hoc comparisons were conducted for each region using Tukey's tests.

All analyses were conducted in R (version 3.5.3). We used the `glmer` function from package *lme4* to fit the generalized linear mixed-effects models. Decomposition models were fit with a gamma distribution and identity link function. We checked model residuals for violation of model assumptions and to investigate the suitability of the chosen distribution (i.e. deviance residuals vs. theoretical quantiles), dispersion and heteroscedasticity, using package *DHARMA* (Supplementary Information 1). To stabilize parameter estimation, we standardized mean light by dividing it by 100, so it matched the scale of the other predictor variables. We used likelihood ratio tests with single-term deletions to assess the importance of each fixed effect predictor in the models. Relationships between the most important predictor variables and decomposition rates were illustrated with package *visreg*, which shows the relationship between a single predictor and the model outcome while holding the other predictors constant⁶⁸.

Declarations

Acknowledgements:

We thank Eva Ramirez-Llodra for leading the KELCO workshop in Oslo where this idea was conceived. We thank Heather Denham and the Wernberg lab for technical assistance in constructing and shipping the equipment. Emanuel Almada, Enora Bocher, Tibor Dorsaz, Stein Fredriksen, Chris Guo, Laurent Lévèque, Arley Muth, Brian Ulaski and Joseph Grace provided field assistance. This study was funded by the Norwegian Blue Forest Network. KFD was also supported by the Australian Research Council (DP190100058, DE190100692) and the National Science and Engineering Research Council of Canada. KHD by BOEM Award M12AS0001. D.S. was supported by a UKRI Future Leaders Fellowship (MR/S032827/1). TW was supported by the Australian Research Council (DP170100023, DP190100058). KH by Norwegian Research Council #267536. PJM was supported by a NERC Newton Fund grant (NE/S011692/1). LEJ and IG by a Canadian NSERC Discovery Grant. FdB & DD were supported by the Brittany Regional Council and the French Government through the National Research Agency with regards to the investment expenditure program IDEALG (reference: ANR-10-BTBR-04).

Author contributions: DS, KFD, KK, TW, MFP, KMN, MB, PJM, KH, and KHD conceived the study. KFD, TW, DS, and KK designed the experiment. CF and DY led the stable isotope analyses. KFD collated and analyzed the data, made the figures and led the writing of the manuscript. TW, CJF, DS, JB, KK, MP, and PJM and provided statistical advice on data analysis and helped interpret the results. All authors funded, organized and/or participated in the fieldwork, edited the manuscript and agreed to its publication in its current form.

Additional information: Supplementary material accompanies this paper.

Competing interests: The authors declare no competing interests.

References

1. Snelgrove, P. V. R. *et al.* Global carbon cycling on a heterogeneous seafloor. *Trends Ecol. Evol.* **33**, 96–105 (2018).
2. Bianchi, T. S. *et al.* Centers of organic carbon burial and oxidation at the land-ocean interface. *Org. Geochem.* **115**, 138–155 (2018).
3. Ciais, P. *et al.* in *Climate Change 2013: The Physical Science Basis. Contribution of Working Group I to the Fifth Assessment Report of the Intergovernmental Panel on Climate Change* (Cambridge University Press, 2013).
4. Arnosti, C., Steen, A. D., Ziervogel, K., Ghobrial, S. & Jeffrey, W. H. Latitudinal gradients in degradation of marine dissolved organic carbon. *PLoS One* **6**, e28900 (2011).
5. Qin, S. *et al.* Temperature sensitivity of SOM decomposition governed by aggregate protection and microbial communities. *Sci. Adv.* **5**, eaau1218 (2019).
6. Davidson, E. A. & Janssens, I. A. Temperature sensitivity of soil carbon decomposition and feedbacks to climate change. *Nature* **440**, 165–173 (2006).
7. Xue, K. *et al.* Tundra soil carbon is vulnerable to rapid microbial decomposition under climate warming. *Nat. Clim. Chang.* **6**, 595–600 (2016).
8. Silver, W. L. & Miya, R. K. Global patterns in root decomposition: Comparisons of climate and litter quality effects. *Oecologia* **129**, 407–419 (2001).
9. Krause-Jensen, D. & Duarte, C. M. Substantial role of macroalgae in marine carbon sequestration. *Nat. Geosci.* **9**, 737–742 (2016).
10. Barrón, C., Apostolaki, E. T. & Duarte, C. M. Dissolved organic carbon fluxes by seagrass meadows and macroalgal beds. *Front. Mar. Sci.* **1**, 42 (2014).
11. Krause-Jensen, D. *et al.* Sequestration of macroalgal carbon: the elephant in the Blue Carbon room. *Biol. Lett.* **14**, 20180236 (2018).
12. Bird, M. I., Chivas, A. R. & Head, J. A latitudinal gradient in carbon turnover times in forest soils. *Nature* **381**, 143–146 (1996).
13. Bradford, M. A. *et al.* Managing uncertainty in soil carbon feedbacks to climate change. *Nat. Publ. Gr.* **6**, (2016).
14. Zhou, T., Shi, P., Hui, D. & Luo, Y. Global pattern of temperature sensitivity of soil heterotrophic respiration (Q₁₀) and its implications for carbon-climate feedback. *J. Geophys. Res.* **114**, G02016 (2009).
15. Tang, J. & Riley, W. Weaker soil carbon–climate feedbacks resulting from microbial and abiotic interactions. *Nat. Clim. Chang.* (2015).
16. Lutz, M., Dunbar, R. & Caldeira, K. Regional variability in the vertical flux of particulate organic carbon in the ocean interior. *Global Biogeochem. Cycles* **16**, 11-1-11–18 (2002).

17. Kirschbaum, M. U. F. The temperature dependence of organic-matter decomposition—still a topic of debate. *Soil Biol. Biochem.* **38**, 2510–2518 (2006).
18. Sitch, S. *et al.* Evaluation of ecosystem dynamics, plant geography and terrestrial carbon cycling in the LPJ dynamic global vegetation model. *Glob. Chang. Biol.* **9**, 161–185 (2003).
19. Crowther, T. W. *et al.* Quantifying global soil carbon losses in response to warming. *Nature* **540**, 104–108 (2016).
20. Krumhansl, K. & Scheibling, R. Production and fate of kelp detritus. *Mar. Ecol. Prog. Ser.* **467**, 281–302 (2012).
21. Wernberg, T., Krumhansl, K. A., Filbee-Dexter, K. & Pedersen, M. F. in *World Seas: An Environmental Evaluation, Vol III: Ecological Issues and Environmental Impacts* (ed. Sheppard, C.) (Academic Press, 2019).
22. Assis, J. *et al.* Major shifts at the range edge of marine forests: the combined effects of climate changes and limited dispersal. *Sci. Rep.* **7**, 44348 (2017).
23. Martínez, B. *et al.* Distribution models predict large contractions of habitat-forming seaweeds in response to ocean warming. *Divers. Distrib.* **24**, 1350–1366 (2018).
24. Krumhansl, K. A. *et al.* Global patterns of kelp forest change over the past half-century. *Proc. Natl. Acad. Sci.* **113**, 13785–13790 (2016).
25. Wernberg, T. *et al.* An extreme climatic event alters marine ecosystem structure in a global biodiversity hotspot. *Nat. Clim. Chang.* **3**, 78–82 (2013).
26. Bolton, J. J., Anderson, R. J., Smit, A. J. & Rothman, M. D. South African kelp moving eastwards: The discovery of *Ecklonia Maxima* (Osbeck) *papenfuss* at De Hoop Nature Reserve on the South Coast of South Africa. *African J. Mar. Sci.* **34**, 147–151 (2012).
27. Filbee-Dexter, K., Wernberg, T., Fredriksen, S., Norderhaug, K. M. & Pedersen, M. F. Arctic kelp forests: Diversity, resilience and future. *Glob. Planet. Change* **172**, 1–14 (2019).
28. Bartsch, I. *et al.* Changes in kelp forest biomass and depth distribution in Kongsfjorden, Svalbard, between 1996–1998 and 2012–2014 reflect Arctic warming. *Polar Biol.* **39**, 2021–2036 (2016).
29. Friedlander, A. M. *et al.* Kelp forests at the end of the earth: 45 years later. *PLoS One* **15**, e0229259 (2020).
30. Norderhaug, K. M. & Christie, H. Secondary production in a *Laminaria hyperborea* kelp forest and variation according to wave exposure. *Estuar. Coast. Shelf Sci.* **95**, 135–144 (2011).
31. Berner, R. A. The long-term carbon cycle, fossil fuels and atmospheric composition. *Nature* **426**, 323–326 (2003).
32. Ortega, A. *et al.* Important contribution of macroalgae to oceanic carbon sequestration. *Nat. Geosci.* **12**, 748–754 (2019).
33. Filbee-Dexter, K., Wernberg, T., Ramirez-Llodra, E., Norderhaug, K. M. & Pedersen, M. F. Movement of pulsed resource subsidies from shallow kelp forests to deep fjords. *Oecologia* **187**, 291–304 (2018).

34. Queirós, A. M. *et al.* Connected macroalgal-sediment systems: blue carbon and food webs in the deep coastal ocean. *Ecol. Monogr.* (2019). doi:10.1002/ecm.1366
35. Smith, R. W., Bianchi, T. S., Allison, M., Savage, C. & Galy, V. High rates of organic carbon burial in fjord sediments globally. *Nat. Geosci.* **8**, 450–453 (2015).
36. Filbee-Dexter, K. *et al.* Carbon export is facilitated by sea urchins transforming kelp detritus. *Oecologia* **192**, 213–225 (2020).
37. Wernberg, T. & Filbee-Dexter, K. Missing the marine forest for the trees. *Mar. Ecol. Prog. Ser.* 209–215 (2019). doi:10.3354/meps12867
38. Ducklow, H., Steinberg, D. & Buesseler, K. Upper ocean carbon export and the biological pump. *Oceanography* **14**, 50–58 (2001).
39. Falkowski, P. *et al.* The global carbon cycle: A test of our knowledge of earth as a system. *Science* **290**, 291–296 (2000).
40. Schemske, D. W., Mittelbach, G. G., Cornell, H. V., Sobel, J. M. & Roy, K. Is there a latitudinal gradient in the importance of biotic interactions? *Annu. Rev. Ecol. Evol. Syst.* **40**, 245–269 (2009).
41. Moles, A. T., Bonser, S. P., Poore, A. G. B., Wallis, I. R. & Foley, W. J. Assessing the evidence for latitudinal gradients in plant defence and herbivory. *Funct. Ecol.* **25**, 380–388 (2011).
42. Boyero, L. *et al.* A global experiment suggests climate warming will not accelerate litter decomposition in streams but might reduce carbon sequestration. *Ecol. Lett.* **14**, 289–294 (2011).
43. Poore, A. G. B. *et al.* Global patterns in the impact of marine herbivores on benthic primary producers. *Ecol. Lett.* **15**, 912–922 (2012).
44. Weston, N. B. & Joye, S. B. Temperature-driven decoupling of key phases of organic matter degradation in marine sediments. *Proc. Natl. Acad. Sci. U. S. A.* **102**, 17036–17040 (2005).
45. Hancke, K. & Glud, R. Temperature effects on respiration and photosynthesis in three diatom-dominated benthic communities. *Aquat. Microb. Ecol.* **37**, 265–281 (2004).
46. Wall, D. H. *et al.* Global decomposition experiment shows soil animal impacts on decomposition are climate-dependent. *Glob. Chang. Biol.* **14**, 2661–2677 (2008).
47. Wernberg, T. & Filbee-Dexter, K. Grazers extend blue carbon transfer by slowing sinking speeds of kelp detritus. *Sci. Rep.* **8**, 17180 (2018).
48. Pessarrodona, A., Moore, P. J., Sayer, M. D. J. & Smale, D. A. Carbon assimilation and transfer through kelp forests in the NE Atlantic is diminished under a warmer ocean climate. *Glob. Chang. Biol.* **24**, 4386–4398 (2018).
49. Trevathan-Tackett, S. M. *et al.* Comparison of marine macrophytes for their contributions to blue carbon sequestration. *Ecology* **96**, 3043–3057 (2015).
50. de Bettignies, F. *et al.* Degradation dynamics and processes associated with the accumulation of *Laminaria hyperborea* kelp fragments: an in situ experimental approach. *J Phycol* **in revisio**, (2020).
51. Smale, D. A., Moore, P. J., Queirós, A. M., Higgs, N. D. & Burrows, M. T. Appreciating interconnectivity between habitats is key to blue carbon management. *Front. Ecol. Environ.* **16**, 71–73 (2018).

52. Couteaux, M. M., Bottner, P. & Berg, B. Litter decomposition, climate and litter quality. *Trends in Ecology & Evolution* **10**, 63–66 (1995).
53. Enríquez, S., Duarte, C. M. & Sand-Jensen, K. Patterns in decomposition rates among photosynthetic organisms: the importance of detritus C:N:P content. *Oecologia* **94**, 457–471 (1993).
54. Norderhaug, K. M., Fredriksen, S. & Nygaard, K. Trophic importance of *Laminaria hyperborea* to kelp forest consumers and the importance of bacterial degradation to food quality. *Mar. Ecol. Prog. Ser.* **255**, 135–144 (2003).
55. Krumhansl K.A. & Scheibling R.E. Detrital subsidy from subtidal kelp beds is altered by the invasive green alga *Codium fragile* ssp. *fragile*. *Mar. Ecol. Prog. Ser.* **456**, 73–85 (2012).
56. Feehan, C. J., Grace, S. P. & Narvaez, C. A. Ecological feedbacks stabilize a turf-dominated ecosystem at the southern extent of kelp forests in the Northwest Atlantic. *Sci. Rep.* **9**, 7078 (2019).
57. Tuya, F. *et al.* Patterns of landscape and assemblage structure along a latitudinal gradient in ocean climate. *Mar. Ecol. Prog. Ser.* **466**, 9–19 (2012).
58. Raybaud, V. *et al.* Decline in kelp in west Europe and climate. *PLoS One* **8**, e66044 (2013).
59. Smale, D. A., Wernberg, T., Yunnice, A. L. E. & Vance, T. The rise of *Laminaria ochroleuca* in the Western English Channel (UK) and comparisons with its competitor and assemblage dominant *Laminaria hyperborea*. *Mar. Ecol.* **36**, 1033–1044 (2015).
60. Pessarrodona, A., Foggo, A. & Smale, D. A. Can ecosystem functioning be maintained despite climate-driven shifts in species composition? Insights from novel marine forests. *J. Ecol.* **107**, 91–104 (2019).
61. Burt, J. M. *et al.* Sudden collapse of a mesopredator reveals its complementary role in mediating rocky reef regime shifts. (2018). doi:10.1098/rspb.2018.0553
62. Konar, B. & Estes, J. A. The stability of boundary regions between kelp forests and deforested areas. *Ecology* **84**, 174–185 (2003).
63. Rogers-Bennett, L. & Catton, C. A. Marine heat wave and multiple stressors tip bull kelp forest to sea urchin barrens. *Sci. Rep.* **9**, 1–9 (2019).
64. Krause-Jensen, D. & Duarte, C. M. Expansion of vegetated coastal ecosystems in the future Arctic. *Front. Mar. Sci.* **1**, (2014).
65. Bonsell, C. & Dunton, K. H. Long-term patterns of benthic irradiance and kelp production in the central Beaufort Sea reveal implications of warming for Arctic inner shelves. *Prog. Oceanogr.* (2018). doi:10.1016/j.pocean.2018.02.016
66. Boulton, A. J. & Boon, P. I. A review of methodology used to measure leaf litter decomposition in lotic environments: Time to turn over an old leaf? *Mar. Freshw. Res.* **42**, 1–43 (1991).
67. Zhang, D., Hui, D., Luo, Y. & Zhou, G. Rates of litter decomposition in terrestrial ecosystems: global patterns and controlling factors. *J. Plant Ecol.* **1**, 85–93 (2008).
68. Breheny, P. & Burchett, W. *Visualization of Regression Models Using visreg.*

Tables

Table 1. Summary of generalized linear mixed-effects models (GLMM) relating the decomposition (% d-1) of kelp detritus to environmental conditions and tissue properties at 12 regions of the northern hemisphere. Temperature (average and range) is temperature at the seafloor over the duration of the experiment. Light is average light (Lux) over the first 2 weeks of the experiment. The % carbon is the initial carbon content in the kelp detritus, and water movement is average g forces within the cages over the experiment. GLMMs are with gamma distribution and identity link function. Model 1 uses the full dataset (n = 12 regions) with predictors temperature (range, average), light and species, and model 2 uses a subset of the data (n = 9 regions) with additional predictors % carbon content and water movement, because these variables were not obtained at all 12 regions. Importance of fixed effects parameters were evaluated using likelihood ratio tests with single-term deletions. Shown for each deletion are percentage of deviance explained (%De) and Chi-squared statistic used to compare model with deletion to full model. Site and region represent random effects.

Model 1				
Fixed effects	Log-Likelihood	% De	Chi²	p
All parameters	-11,470			
Average temperature	-15,208	32.8	7,47	0,006
Temperature range	-11,48	0,31	0,02	0,887
Light	-11,640	1.66	0,33	0,566
Species	-14,966	28.1	6,45	0,011
Random effects	N	Variance	SD	
(1 Site:Region)	34	0.014	0.118	
(1 Region)	12	0.156	0.395	
Residual		0.032	0.178	

Model 2				
Fixed Effects	Log-Likelihood	% De	Chi²	P
All parameters	-10.33			
Average temperature	-15.24	47.5	9.82	0.002
Temperature range	-10.81	4.6	0.94	0.332
% carbon	-13.53	30.9	6.39	0.012
Light	-10.55	2.1	0.43	0.510
Water movement	-10.46	1.2	0.24	0.621
Species	-15.26	47.7	9.85	0.002
Random effects	N	Variance	SD	
(1 Site:Region)	26	0.020	0.143	
(1 Region)	9	0.090	0.300	
Residual		0.024	0.154	

Figures

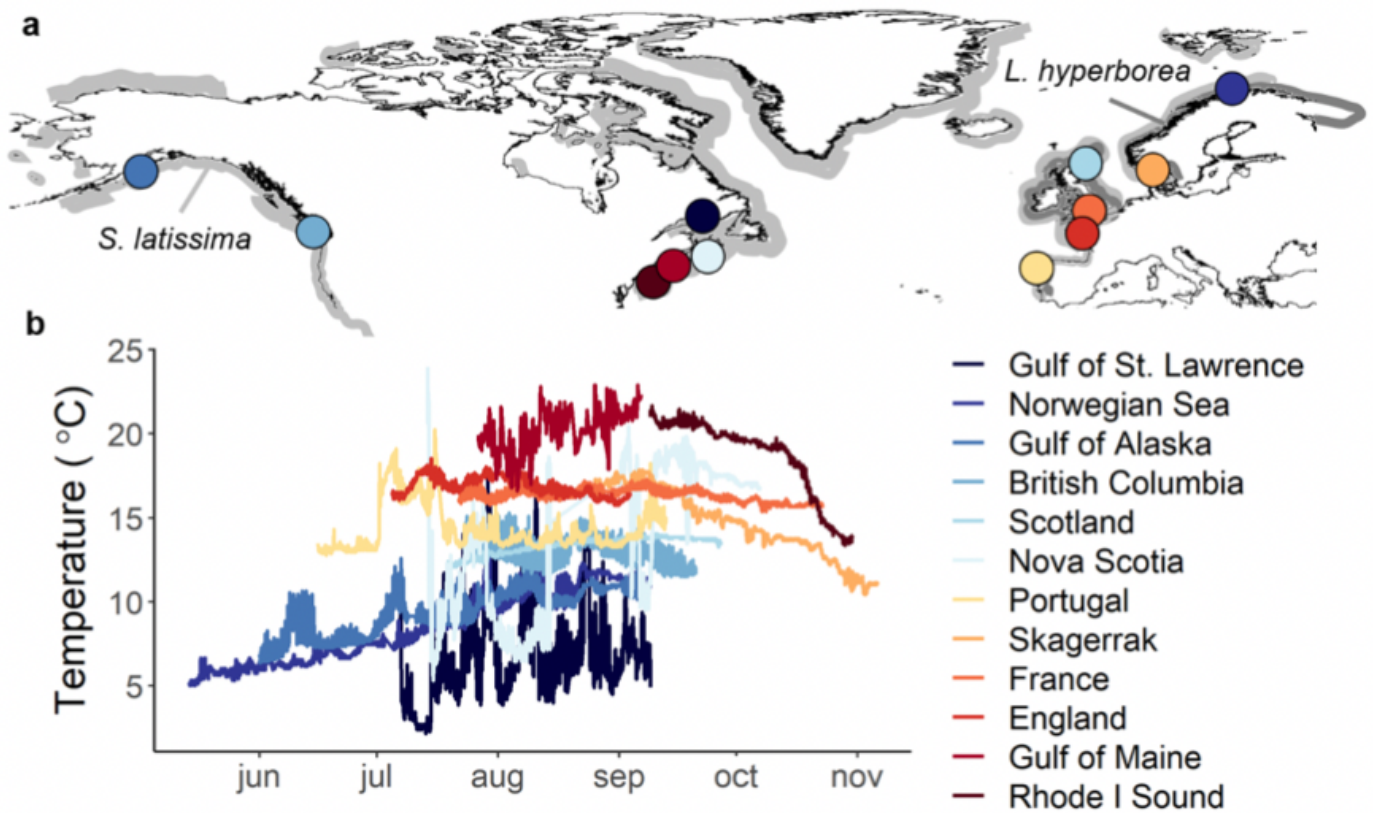


Figure 1

Study regions and temperatures. Map of study regions (a) and temperature records (b) over the duration of the experiment. Distributions of *Saccharina latissima* and *Laminaria hyperborea* kelps, modified from 37, are shown in light and dark gray respectively. Additional details in Supplementary Table 1. Note: The designations employed and the presentation of the material on this map do not imply the expression of any opinion whatsoever on the part of Research Square concerning the legal status of any country, territory, city or area or of its authorities, or concerning the delimitation of its frontiers or boundaries. This map has been provided by the authors.

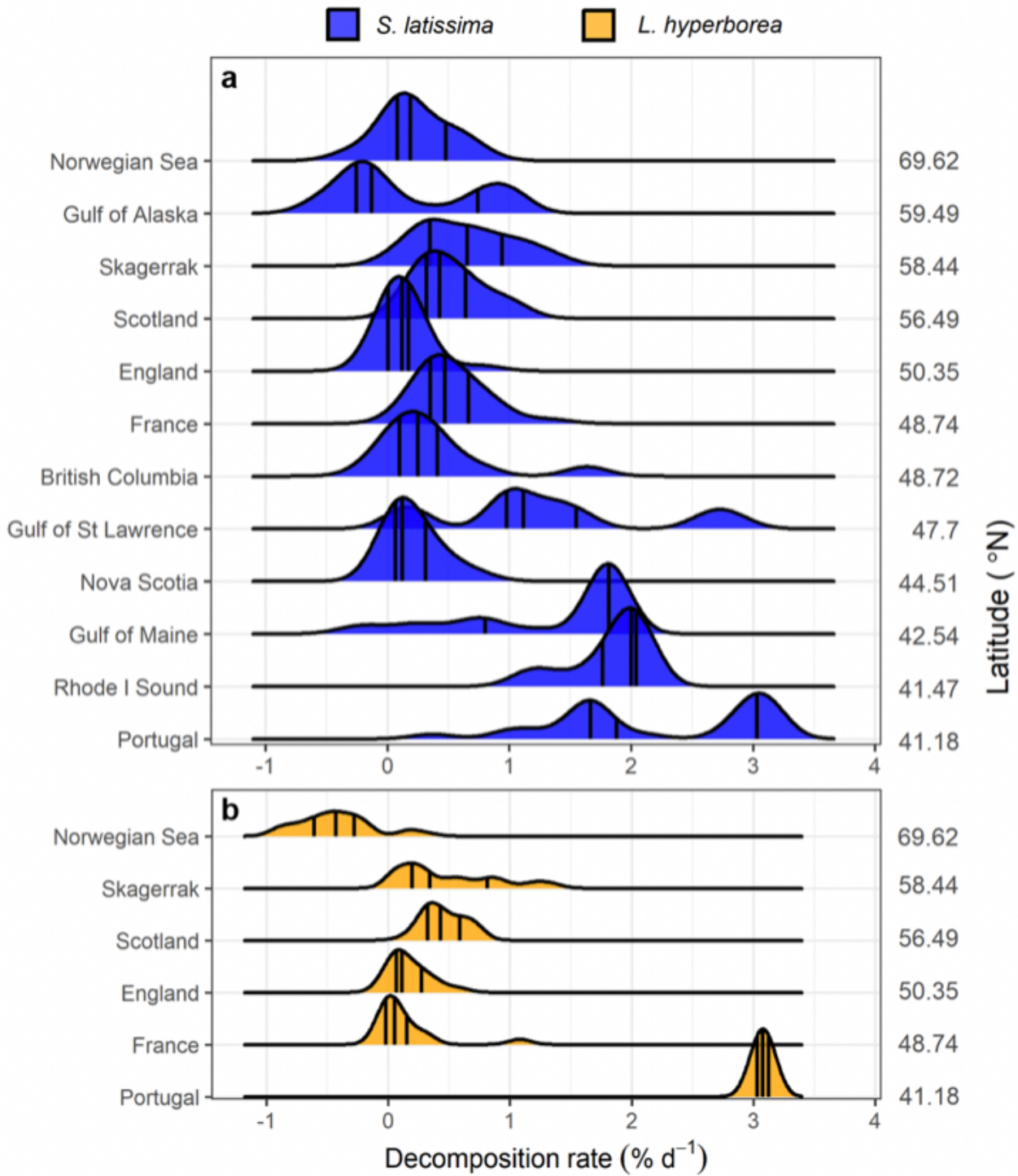


Figure 2

Kelp decomposition rates. Probability density functions of decomposition rates of (a) *Saccharina latissima* and (b) *Laminaria hyperborea* throughout the northern hemisphere. Curves show frequency of observations, pooled across sites in each region and ordered by latitude. Black middle lines show medians, and outer lines show the 25th and 75th quantiles. Y axes units are the proportion of observations, ranging from 0 to 0.18 (a) and from 0 to 0.9 (b) for each site.

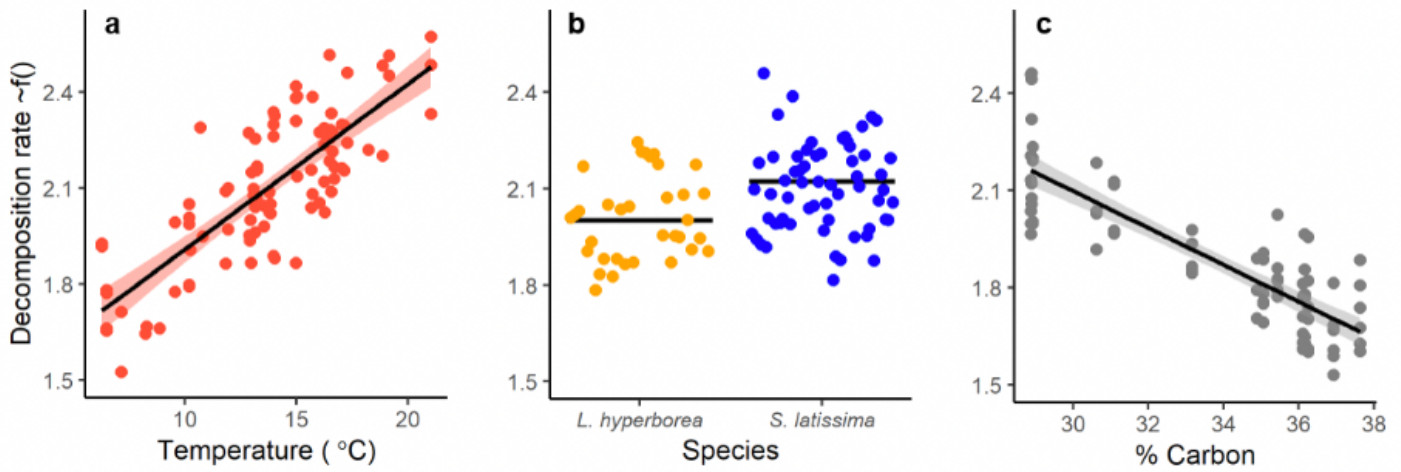


Figure 3

Drivers of decomposition. Relationships between kelp decomposition rate (% d⁻¹) and significant predictor variables in generalized linear models: (a) average water temperature during the experiment, (b) species, and (c) initial % carbon content, from the generalized linear mixed effect models, with all other variables in the model held fixed. Black lines are the expected value from the model, shaded error bar (a & c) is confidence interval, and points are partial residuals for each sampling time at each site. Relationship with % carbon is based on a subset of 9 out of 12 regions for which data existed.

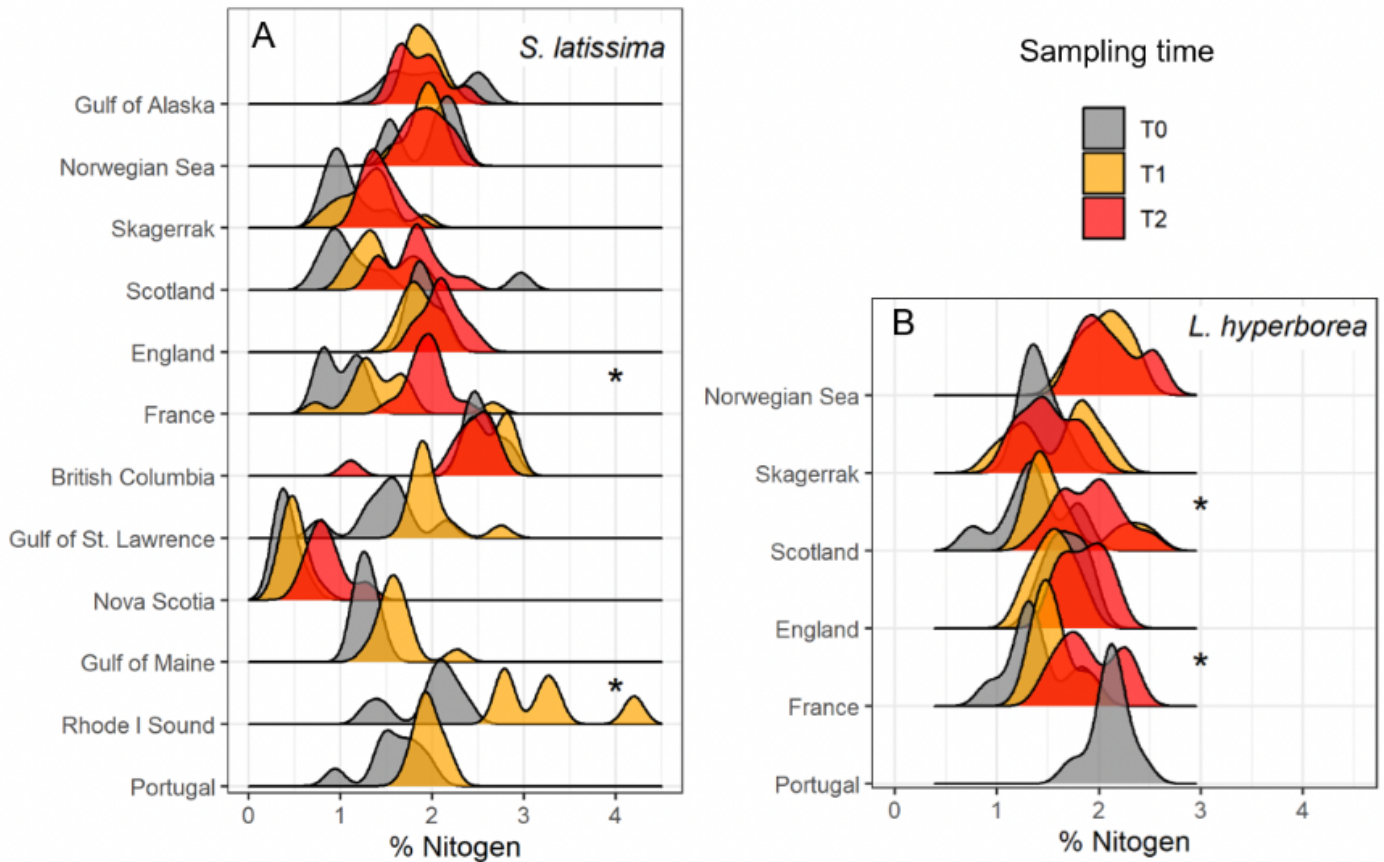


Figure 4

Change in detritus quality. Total nitrogen content in kelp detritus over the experiment for *Saccharina latissima* and *Laminaria hyperborea*. Data are frequency measures of % nitrogen from tissue samples taken at the onset of the experiment (T0), the first sampling time (T1) and the final sampling (T2). Y axes units are the proportion of observations. Measures are pooled across sites for each region and ordered by decreasing latitude. Values are missing for later samplings in some regions because insufficient biomass remained for analysis at the time of sampling (* denotes statistical significance, post hoc tests in Supplementary Table 3).

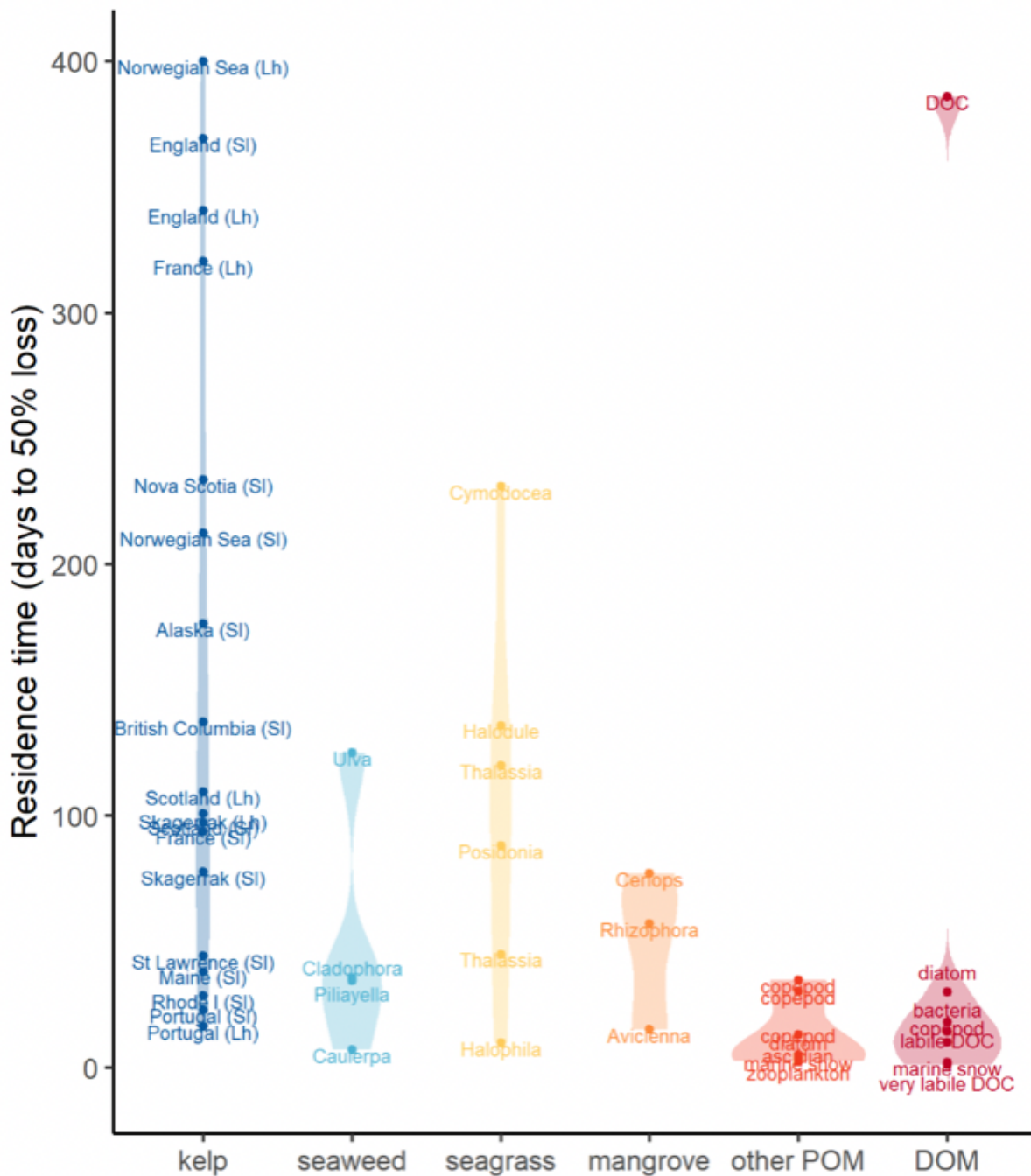


Figure 5

Figure 4. Residence time of marine detritus. Residence times (days to 50% decomposition) reported for different types of marine detritus, including kelps from our study regions (SI = *Saccharina latissima*; Lh = *Laminaria hyperborea*) and measures reported in the literature for other seaweeds, seagrass, mangrove detritus (leaf), other particulate organic material (POM) and dissolved organic material (DOM) (Supplementary Table 4). POM consist of zooplankton debris, feces, fauna casings and marine snow.

DOM is labile DOC or DOM released from zooplankton debris or marine snow during incubations. Refractory DOC is not shown and residence times for this organic carbon pool range from years to decades or more.

Supplementary Files

This is a list of supplementary files associated with this preprint. Click to download.

- [Supplementaryinformationv1.docx](#)